IEEE Access
Multidisciplinary | Rapid Review | Open Access Journal

Received May 27, 2018, accepted June 27, 2018, date of publication July 2, 2018, date of current version July 25, 2018.

Digital Object Identifier 10.1109/ACCESS.2018.2852368

Blind Nonlinear Self-Interference Cancellation for Wireless Full-Duplex Transceivers

XIN QUAN[1], (Member, IEEE), YING LIU[1], (Member, IEEE), DONG CHEN[2], SHIHAO SHAO[1], (Member, IEEE), YOUXI TANG[1], AND KANG KANG[2], (Member, IEEE)

[1]National Key Laboratory of Science and Technology on Communications, University of Electronic Science and Technology of China, Chengdu 611731, China
[2]School of Electronic Engineering, University of Electronic Science and Technology of China, Chengdu 611731, China

Corresponding author: Ying Liu (liuying850613@uestc.edu.cn)

This work was supported in part by the National Natural Science Foundation of China under Grant 61701075, Grant 61771107, Grant 61771115, Grant 61531009, and Grant 61471108, in part by the National Science and Technology Major Project under Grant 2016ZX03001009, in part by the Project funded by the China Postdoctoral Science Foundation, and in part by the Fundamental Research Funds for the Central Universities.

ABSTRACT As the transmission power increases for high-power full-duplex (FD) communications, the nonlinear effects of the transmit chain become more significant, resulting in severe nonlinear self-interference (SI) at the receiver of the FD transceiver and hence demodulation performance degradation for the desired signal from a remote user. In this paper, a blind nonlinear SI cancellation method, which consists of a cancellation stage and a recovery stage, is proposed to cancel the nonlinear SI along with the linear SI signal for an orthogonal frequency division multiplexed (OFDM)-modulated FD transceiver. By taking the advantage of two symbols on adjacent subcarriers received in one OFDM symbol, the cancellation stage cancels both the linear SI and its nonlinear SI components of the received signal without estimating the transmitter nonlinearity as well as the SI channel response. Subsequently, the recovery stage is performed on the resulting signal of the cancellation stage to eliminate any impacts on the desired signal. Simulations are performed on a nonlinear model extracted from a practical class AB power amplifier with transmission power ranging from 10 to 30 dBm to demonstrate different nonlinear distortions. The effectiveness of the proposed nonlinear cancellation method is verified in terms of the computation complexity, the cancellation capability for the SI signal, and the bit error rate of the desired signal.

INDEX TERMS Blind cancellation, full-duplex communication, power amplifier nonlinear distortion, self-interference cancellation.

I. INTRODUCTION

Full-duplex (FD) wireless communication is technology that enables a radio frequency (RF) transceiver to simultaneously transmit and receive signals using the same carrier frequency thus has gained much attention both in academia and industry [1], [2]. By applying this technology, the spectrum efficiency of a communication system is dramatically improved, and can even be doubled in theory [3], [4]. However, one of the biggest challenges to apply FD technology in practice is to cancel the self-interference (SI) signal introduced by the transmitted signal at the local receiver [5]. For instance, for an FD transceiver of 20 MHz bandwidth, the SI signal at the local receiver would be 100 dB above the receiver noise floor when transmitting at 20 dBm, due to the limited propagation isolation between the local transmit and receive antennas (e.g., 15–20 dB isolation for a single-antenna FD transceiver using a circulator or 20–40 dB for a dual-antenna FD transceiver with limited distance between the transmit and receive antennas [7]–[11]).

For typical FD communication scenarios with low transmission power, some successful strategies have been employed to suppress the SI close to the receiver noise floor, demonstrating good cancellation performance in theory and in laboratory experiments [8]–[12]. In these scenarios, an analog cancellation and a digital cancellation are performed in a consecutive manner to achieve a maximum amount of cancellation for the SI signal. The analog cancellation is usually deployed at the receiver front end to first mitigate the strong SI signal to prevent saturating the analog-to-digital converter (ADC) of the local receiver and ensure the desired signal from a remote user could be captured by the local receiver. Subsequently, in the digital domain, the digital

SI cancellation scheme is deployed to further suppress the residual SI to close to the receiver noise floor and ensure the desired signal can be effectively demodulated without performance degradation.

However, in practice for high-power FD applications, the cancellation amount (cancellation capability) needed to realize FD communications becomes even larger, and hence requirement for each cancellation SI stage becomes more stringent. Particularly, for high-power FD transceiver, the inherent nonlinearity of the power amplifier (PA) introduces strong nonlinear distortion for the SI signal. As a consequence, the SI signal usually consists of the linear components (i.e., the delayed and attenuated copies of the transmitted signal) and the nonlinear components introduced by the power amplifier (PA) nonlinear distortions [3], [13]. As the transmission power further increases, the nonlinear effects of the transmitter becomes even more significant, thus the nonlinear SI components becomes more severe and no longer ignorable [14], [15]. As stated in work [13], even after the analog and digital SI cancellations, the power of the nonlinear SI components can still be 20 dB above the desired signal. Therefore, the nonlinear SI signal needs to be seriously considered and effectively suppressed.

To account for the nonlinear distortion, recently, some PA modeling-based nonlinear cancellation methods are proposed [13]–[17]. In [13], [15], and [16], the authors use a general model to approximate the non-linear function with Taylor series expansion. While in [17], the authors use a parallel Hammerstein for discrete-time baseband modeling of the nonlinear PA model instead. These methods require an extra training process to estimate the PA nonlinear coefficients before performing digital SI cancellation. High computation complexity would be included to the training process for coefficients estimation (e.g., using least-square (LS) algorithm for model estimation) [18]. Additionally, this training process also requires adaptation capability to cope with the variation of the PA nonlinear behavior, which is sensitive to the statistics of the transmitted signal, the working temperature of the environments, and the supply voltage variations, resulting in complicated structure for implementation.

Motivated by these issues above, in this work, a simple architecture based on blind cancellation is proposed for an orthogonal frequency division multiplexed (OFDM)-modulated FD transceiver experiencing nonlinear distortions without any training process. This architecture first uses a simple cancellation process to cancel both the linear and nonlinear SI components by combining the consecutively received symbols on adjacent subcarriers in one OFDM symbol. Subsequently, to eliminate the impacts of the cancellation process on the desired signal, a recovery process is deployed on the resulting signal of the SI cancellation stage. During the cancellation and recovery processes, it is not required to estimate the linear SI channel response and the PA nonlinear model coefficients, resulting in low computation complexity and simple structure for implementation, which is the core contribution of this approach. To the best of our knowledge, this is the first work to cancel the nonlinear SI components with such blind cancellation approach in FD systems.

In order to assess the validity of this approach, simulations using parameters extracted from practical RF devices of a real FD transceiver are explicitly performed. The computation complexity, the cancellation capability of the SI signal, and the bit error rate (BER) of the desired signal are compared with the conventional linear SI cancellation [12] and nonlinear SI cancellation [13]. With excellent cancellation capability for the SI signal, the residual SI power after the proposed blind cancellation approach is shown to be quite close to the receiver noise floor. While the BER of the desired signal after blind cancellation approach is shown to be close to the ideal case without any linear or nonlinear SI signals, indicating that the impacts of the blind cancellation on the desired signal is ignorable. The BER, the cancellation capability on the SI signal and the residual SI power are all comparable to the conventional nonlinear SI cancellation method of high computation complexity [13]. Differently, as the proposed blind cancellation approach does not need to estimate the nonlinear PA model coefficients and the linear SI channel response, it demonstrates much lower computation complexity and simpler structure for implementation.

The remainder of this paper is organized as follows. In Section II, the signal model of the considered FD system is introduced. In Section III, the proposed blind SI cancellation scheme is presented, where the SI cancellation and recovery processes are presented in Section III.A and III.B, respectively. Performance analysis on the nonlinear order to be cancelled and the computation complexity are presented in Section IV. Simulation and discussions are presented in Section V. Finally, Section VI concludes this work.

II. SYSTEM MODEL

A. SIGNAL WAVEFORM

An OFDM-modulated FD transceiver employing analog cancellation and digital nonlinear cancellation to suppress the SI signal is shown in Fig. 1. Let us consider a regular OFDM transmitter with N subcarriers of frequencies separated by Δf. The complex envelope of the transmitted OFDM waveform is given as [19]

$$x(t) = \frac{1}{\sqrt{N}} \sum_{k=0}^{N-1} X[k] e^{j2\pi k \Delta f t}, \quad 0 \le t \le T, \tag{1}$$

where $T = 1/\Delta f$ is the useful symbol length, $j = \sqrt{-1}$, and $X[k]$ is the transmitted symbol on the k-th subcarrier $\exp\{j2\pi k \Delta f t\}$. In order to build the OFDM waveform $x(t)$, we take an N-point inverse discrete Fourier transform (IDFT) on the $N \times 1$ signal vector $[X[0], X[1], \cdots, X[N-1]]^T$ to generate the baseband waveform $x(n)$ in time domain, before the digital-to-analog converter (DAC).

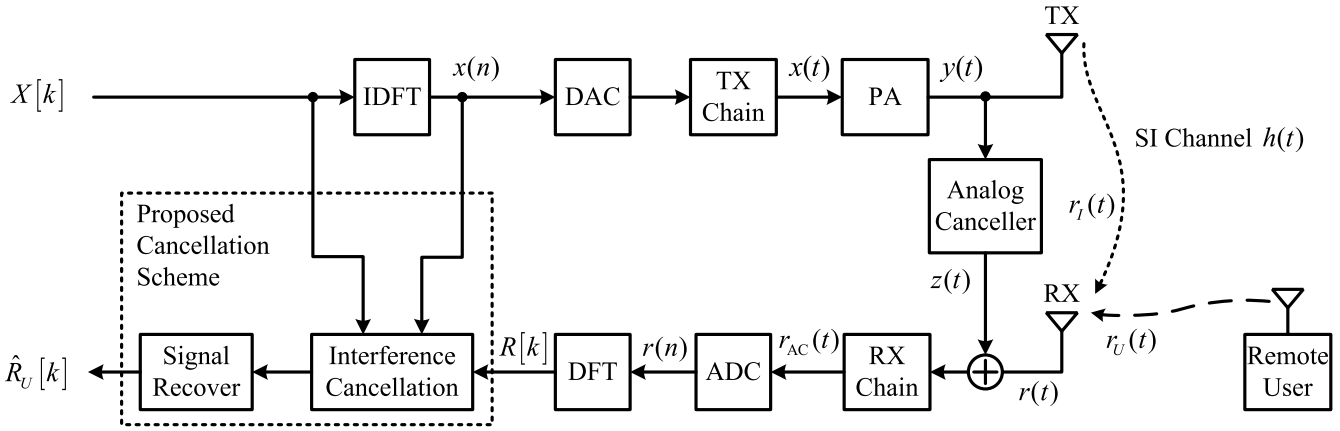

FIGURE 1. Full-duplex transceiver with nonlinear cancellation architecture.

B. PA NONLINEARITY

After OFDM waveform generation, $x(t)$ is then fed to a PA for signal amplification before transmitting over the air. To address the nonlinearity of the transmitter, a memoryless model (MLM) is used here to represent the PA as [20]

$$y(t) = \sum_{m=0}^{M} a_{2m+1}|x(t)|^{2m}x(t), \tag{2}$$

where $x(t)$ and $y(t)$ are the input and output of the PA, respectively, a_{2m+1} is the coefficient of the $(2m+1)$-th order of nonlinearity, and $(2M+1)$ is the maximum nonlinear order.

Notice that during the development of our cancellation algorithm, we only considered a PA model with third-order nonlinearity for simplicity, thus transmitted signal is given as

$$y(t) = a_1x(t) + a_3|x(t)|^2x(t). \tag{3}$$

A more general case with higher nonlinear orders will be discussed in the next section.

C. SI CHANNEL

The channel impulse response between the transmit and the receive antennas, i.e., the SI channel impulse response, is usually given as [6]

$$h(t) = \sum_{i=1}^{L} h_i\delta(t-\tau_i), \tag{4}$$

where L is the total number of multi-path components, h_i is the channel gain for the i-th multi-path component, and $\delta(t-\tau_i)$ is the continuous-time unit impulse function (also known as delta function) with transmission delay τ_i. After propagation through the SI channel, the transmitted signal $y(t)$ becomes an SI signal $r_I(t)$ at the receiver RF front-end as

$$r_I(t) = y(t) \star h(t) = \sum_{i=1}^{L} h_i y(t-\tau_i), \tag{5}$$

where $(\star)$ denotes convolution operation.

Let us consider a single-antenna FD transceiver (or dual-antenna FD transceiver of closely spaced transmit and receive antennas) located in wide open space with few weak reflections. For instance, in a ground-to-air uplink, as the attitude of the unmanned air vehicle allows the transceiver to stay above the ground-based shadowing and obtain line-of-sight (LOS) or near LOS communication channels over a large area [21], [22]. The SI path is the direct leakage path of the circulator (or the clear LOS path between the transmit and receive antennas), while the space multi-path SI paths are much weaker [21]. For simplicity, the associated SI channel between the transmit and receive chains is then characterized as a simple block fading channel. Accordingly, the SI signal at the receiver RF front-end is given as

$$\begin{aligned} r_I(t) &= hy(t-\tau) \\ &= ha_1x(t-\tau) + ha_3|x(t-\tau)|^2x(t-\tau), \end{aligned} \tag{6}$$

where h and τ represent the gain and delay of the SI channel, respectively. It has to be noticed that we neglect the space multi-path SI signals only during the developments of the cancellation algorithm. However, numerical analysis is performed using both strong LOS SI signal and weak multi-path SI reflections.

D. ANALOG CANCELLER MODEL

As the SI signal $r_I(t)$ is much stronger than the desired signal, it would saturate the ADC of the receiver chain and prevent the desired signal from entering the digital domain. Thus, an analog canceller is usually deployed before the ADC sampling process to first reduce the strength of the SI signal. According to the SI channel in (4), the analog canceller is usually composed of multiple taps to account for different multi-path components [12], [13], each of which consists of a fixed delay line, a variable attenuator, and a phase shifter for amplitude and time alignments. In the considered scenario, we only used a single-tap analog canceller for proof-of-concept illustration. The cancelling signal is then simply

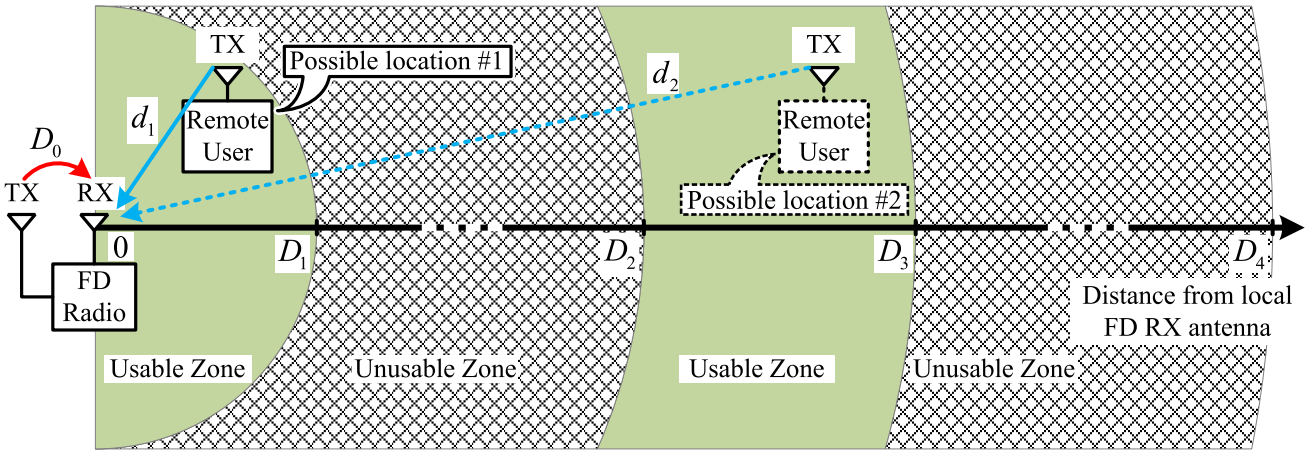

FIGURE 2. Coverage of the full-duplex transceiver with $D_i = D_0 + n \times c \times T_{CP}$, where c is the velocity of electromagnetic wave (light) propagation in free space.

given as

$$z(t) = \alpha y(t-\gamma)e^{j\phi} = wy(t-\gamma), \tag{7}$$

where γ, α, and ϕ represent the delay of the canceller, the gain of the variable attenuator, and the phase value of phase shifter, respectively. $w = \alpha \exp(j\phi)$ is the equivalent complex coefficient of the analog canceller.

After choosing the delay line γ to ensure $\gamma \approx \tau$ and tuning the variable attenuator and phase shifter to ensure $w \approx -h$, the cancelling signal $z(t)$ becomes a copy of the SI signal $r_I(t)$, except with a 180-degree phase shift. As shown Fig. 1, the SI signal can be mitigated by using an adder, which is typically implemented by a RF power combiner.

E. DIGITAL SI CANCELLATION MODEL

At the local receiver chain, the received signal after analog cancellation is given

$$r_{AC}(t) = r(t) - z(t) = r_I(t) + r_U(t) + \eta(t) - z(t), \tag{8}$$

where $\eta(t)$ is the noise of the receiver. With the assumption of symbol level synchronization [23]–[25], the received sequence can be written as

$$r(n) = \beta a_1 x(n) + \beta a_3 |x(n)|^2 x(n) + r_U(n) + \eta(n), \tag{9}$$

where $\beta = h - w$ is the joint impulse response including the SI channel and analog cancellation [4], and $\beta a_1 x(n)$, $\beta a_3 |x(n)|^2 x(n)$, $r_U(n)$, and $\eta(n)$ are the time-domain linear SI, nonlinear SI, signal-of-interest, and receiver noise, respectively. After DFT operation on (9), the received symbols in the frequency domain $\{R[k]\}_{k=0}^{N-1}$ (N is total number of usable subcarriers) are expressed as

$$R[k] = \beta a_1 X[k] + \beta a_3 X_3[k] + R_U[k] + N[k], \tag{10}$$

where $R_U[k]$ is the desired signal and $N[k]$ is the receiver noise in frequency domain. $\beta a_1 X[k]$ and $\beta a_3 X_3[k]$ (with $X_3[k]$ being the resulting signal of DFT operation on $\{|x(n)|^2 x(n)\}$) are the frequency-domain linear SI and nonlinear SI signals to be cancelled.

Note that as the local receiver receives a superposition of the SI signal and the desired signal, the symbol synchronization is guaranteed by the cyclic prefix (CP) insertion. In this considered FD application, it is assumed that the overall relative transmission delay difference between the SI signal $r_I(t)$ and desired signal $r_U(t)$ (denoted as Δ_T) is within the CP length, i.e.,

$$\text{mod}\,(\Delta_T, T_S) \le T_{CP}, \tag{11}$$

where mod (Δ_T, T_S) is the remainder when Δ_T is divided by T_S; $T_S = (N_{CP} + N)/(\Delta f N)$ and $T_{CP} = N_{CP}/(\Delta f N)$ denote one OFDM symbol duration and the CP duration, respectively. This assumption is widely used in current literatures on FD communications, such as [24]–[27], and holds in the following two scenarios. In one scenario, both the local transmitter and the remote user transmit simultaneously towards the local receiver [25], [27]. As shown in Fig. 2, the coverage radius of the FD transceiver d of this scenario is obtained from (11) as

$$D_0 + n \times c \times T_{CP} \le d \le D_0 + (n+1) \times c \times T_{CP}, \tag{12}$$

where c is the velocity of electromagnetic wave (light) propagation in free space and D_0 is the distance between the local transmit and receive antennas. For instance, in a 20-MHz LTE system with $N = 2048$ and $\Delta f = 15$ kHz, the normal CP length is chosen to be $N_{CP} = 144$ (corresponding to $T_{CP} = 4.7$ μs) to cover a range of miles, most suitable for FD applications in urban areas. While the extended CP length is chosen to be $N_{CP} = 512$ (corresponding to $T_{CP} = 16.7$ μs) to cover wider ranges, most suitable for FD applications in suburb areas [18]. In the other scenario, by taking advantage of the uplink synchronization technique (which ensures all active users arrive at the base station synchronously) [28]–[30], the desired signal from the remote user and the SI signal from the local transmitter could arrive at

the local receiver synchronously. The design of the CP length and synchronization process are out of the scope of this work and thus are omitted.

III. BLIND NONLINEARITY CANCELLATION SCHEME

In the digital cancellation, the transmitted symbol $X[k]$ and its 3rd-order nonlinear distortion in frequency domain $X_3[k]$ (both signals are known to the local receiver of the FD transceiver) are used to cancel the linear and nonlinear interference signal in $R[k]$. In the considered FD scenario, the SI channel between the local transmit and receive antennas is block fading (i.e., the SI channel response typically remains almost the same for any two adjacent symbols [31]) while the transmitter response (i.e., the PA nonlinearity) remains unchanged within one OFDM symbol. Based on these two consideration, we can derive a new method to cancel both the linear and nonlinear SI components in the received symbol $R[k]$ by using symbol on the adjacent subcarrier $R[k-1]$, given $R[k]$ and $R[k-1]$ share the same SI channel response h and the same PA nonlinear coefficients within one OFDM symbol.

This method consists of two steps: 1) cancel the linear SI $\beta a_1 X[k]$ and nonlinear SI $\beta a_3 X_3[k]$ in (10), and 2) recover the signal-of-interest $R_U[k]$.

A. INTERFERENCE CANCELLATION

Two steps are deployed consecutively to cancel the linear SI $\beta a_1 X[k]$ and nonlinear SI $\beta a_3 X_3[k]$ in (10).

1) LINEAR SI CANCELLATION

In linear SI cancellation step, we use the transmitted symbol $X[k]$ and the received symbol $R[k]$ to build a cancelling signal $C_1[k]$ for the linear SI as:

$$C_1[k] = \frac{X[k]}{X[k-1]} R[k-1], \quad 2 \le k \le K, \tag{13}$$

where $K \le N$ is the processing length. By subtracting $C_1[k]$ from $R[k]$, the linear SI is cancelled and a resulting signal is given as

$$\begin{aligned} Z[k] &= R[k] - C_1[k] \\ &= \beta a_3 \times A[k] + R_U[k] + N[k] \\ &\quad - \frac{X[k]}{X[k-1]}(R_U[k-1] + N[k-1]), \end{aligned} \tag{14}$$

where $\beta a_3\, A[k]$ represents the overall nonlinear effect introduced by the two adjacent symbols with $A[k]$ defined as

$$A[k] = X_3[k] - \frac{X[k]}{X[k-1]} X_3[k-1]. \tag{15}$$

2) NONLINEAR SI CANCELLATION

One can see from the cancellation result in (14) that the linear SI component $\beta a_1 X[k]$ is cancelled after the linear SI cancellation step, however, the nonlinear SI components $\beta a_3 X_3[k]$ and $\beta a_3 X_3[k-1]$ remain in the resulting signal $Z[k]$. Thus, in order to cancel these nonlinear SI components, a nonlinear SI cancelling signal is built as

$$C_3[k] = \frac{A[k]}{A[k-1]} Z[k-1], \quad 3 \le k \le K. \tag{16}$$

Subsequently, $\beta a_3\, A[k]$ is cancelled by subtracting $C_3[k]$ from $Z[k]$ as

$$\begin{aligned} Z_{lin}[k] &= Z[k] - C_3[k] \\ &= R_U[k] + N[k] + i[k], \end{aligned} \tag{17}$$

where $i[k]$ is the residual interference signal after SI cancellation given as

$$\begin{aligned} i[k] = &-\left(\frac{X[k]}{X[k-1]} + \frac{A[k]}{A[k-1]}\right)(R_U[k-1] + N[k-1]) \\ &+ \frac{X[k]}{X[k-1]} \frac{A[k]}{A[k-1]}(R_U[k-2] + N[k-2]). \end{aligned} \tag{18}$$

We can see from the cancellation result in (17) that the received signal becomes a composite signal consists of three components, i.e., the desired signal $R_U[k]$, the noise signal $N[k]$, and the residual interference signal i[k]. Therefore, by applying the two consecutive cancellations on the received signal $R[k]$, both the linear and nonlinear SI signals are effectively cancelled. However, as observed from the definition of $i[k]$ in (18), the signal-of-interest $R_U[k]$ is also interfered by $R_U[k-1]$ and $R_U[k-2]$, which are introduced from the cancellation process above. Thus, a recovery process is needed to recover $R_U[k]$ from $Z_{lin}[k]$ to eliminate the impacts of the cancellation process.

B. SIGNAL-OF-INTEREST RECOVERY

To recover $R_U[k]$ from $Z_{lin}[k]$, we first rewrite $Z_{lin}[k]$ as

$$Z_{lin}[k] = B[k] - \frac{A[k]}{A[k-1]} B[k-1], \ 3 \le k \le K, \tag{19}$$

where $B[k]$ is defined as

$$B[k] = R_U[k] + N[k] - \frac{X[k]}{X[k-1]}(R_U[k-1] + N[k-1]). \tag{20}$$

In (19), $B[k]$ is an intermediate variable that has an identical form as $Z_{lin}[k]$. Thus, to eventually obtain $R_U[k]$ from the cancelling result $Z_{lin}[k]$, two similar estimation steps are deployed, i.e., 1) estimate $B[k]$ from $Z_{lin}[k]$ by performing a recovery operation on (19) and estimate $R_U[k]$ from $B[k]$ by performing a similar recovery operation on (20).

1) RECOVERY OF $B[K]$

Firstly, we can build a signal $z[k]$ from $Z_{lin}[k]$ in (19) as

$$z[K] = Z_{lin}[K], \quad for\ k = K, \tag{21}$$

$$\begin{aligned} z[k] &= z[k+1] + \frac{A[K]}{A[k]} Z_{lin}[k] \\ &= B[K] - \frac{A[K]B[k-1]}{A[k-1]}, \quad for\ 3 \le k \le K-1, \end{aligned} \tag{22}$$

where the construction of $z[k]$ is performed in the descending order of index k, i.e., k is varying from $K-1$ to 3.

Then, from (21) and (22), the estimate of $B[K]$ is obtained by averaging the $K-2$ symbols $\{z[k]\}_{k=3}^{K-1}$ as

$$\hat{B}[K] = \frac{1}{K-2}\sum_{k=3}^{K} z[k] = B[K] + w[K], \tag{23}$$

where $w[K]$ is the residual interference, introduced to the K-th symbol by this recovery step, given by

$$w[K] = -\frac{A[K]}{(K-2)}\sum_{i=2}^{K-1}\frac{B[i]}{A[i]}. \tag{24}$$

By substituting (23) into (22), we can obtain an estimate of $B[k]$ as

$$\begin{aligned}\hat{B}[k] &= \frac{A[k]}{A[K]}(\hat{B}[K] - z[k+1]) \\ &= B[k] + w[k], \quad 2 \le k \le K.\end{aligned} \tag{25}$$

where $w[k]$ is the residual interference, introduced to the k-th symbol by this recovery step, given by

$$w[k] = -\frac{A[K]}{(K-2)}\sum_{i=2}^{K-1}\frac{B[i]}{A[i]}. \tag{26}$$

Thus, $B[k]$ is estimated from signal $Z_{lin}[k]$, which accomplishes the first recovering step.

2) RECOVERY OF $R_U[K]$

Similarly, in this recovery step, we build $b[k]$ from (23) and (25) as

$$b[K] = \hat{B}[K] = R_U[K] + N[K] + w[K], \quad for\ k = K, \tag{27}$$

$$\begin{aligned}b[k] &= b[k+1] + \frac{X[K]}{X[k]}\hat{B}[k] \\ &= R_U[K] + N[K] + \sum_{i=k}^{K}\frac{X[K]w[i]}{X[i]} \\ &\quad - \frac{X[K]}{X[k-1]}(R_U[k-1] + N[k-1]), \quad 2 \le k \le K-1,\end{aligned} \tag{28}$$

where the construction of $b[k]$ is also performed in the descending order of index k, i.e., k is varying from $K-1$ to 2. Then, the estimate of $R_U[K]$ is obtained by averaging the $K-1$ symbols $\{b[k]\}_{k=2}^{K-1}$ as

$$\hat{R}_U[K] = \frac{1}{K-1}\sum_{k=2}^{K} b[k] = R_U[K] + N[K] + v[K], \tag{29}$$

where notation $v[K]$ is the residual interference, introduced to the K-th symbol, calculated as

$$v[K] = -\frac{X[K]}{K-1}\sum_{i=1}^{K-1}\frac{R_U[i]+N[i]}{X[i]} + \frac{X[K]}{K-1}\sum_{i=2}^{K}(i-1)\frac{w[i]}{X[i]}.$$

Finally, by substituting (29) into (27), the estimate of $R_U[k]$ is obtained as

$$\begin{aligned}\hat{R}_U[k] &= \frac{X[k]}{X[K]}(\hat{R}_U[K] - b[k+1]) \\ &= R_U[k] + N[k] + v[k],\ 1 \le k \le K-1,\end{aligned} \tag{30}$$

where notation $v[k]$ is the residual interference, introduced to the k-th symbol, calculated as

$$v[k] = \frac{X[k]}{X[K]}v[K] - X[k]\sum_{i=k+1}^{K}\frac{w[i]}{X[i]}, \quad 1 \le k \le K-1,$$

which also represents the overall effect of the residual interferences of the proposed cancellation and recovery approach. Therefore, at this stage, the desired signal $R_U[k]$ is recovered as $\hat{R}_U[k]$ and can be fed to a conventional demodulator for further data processing.

IV. PERFORMANCE ANALYSIS

A. NONLINEARITY ORDER FOR CANCELLATION

It should be noted that during the development of this cancellation algorithm, we only considered a PA model with third-order nonlinearity for simplicity. Actually, this cancellation algorithm could be easily extended to cover a more general PA model with higher nonlinear orders. Notice that as the cancellation is operated in a totally blind manner, we do not have any prior information about the nonlinear characteristics of the PA. However, we can still reasonably assume knowledge of the maximum nonlinear order, M, as did in many literatures on PA modeling [6], [34] and linearization [20], [35]. Accordingly, we can perform interference cancellation for each potential nonlinear order of the PA in a successive way by using (16) and (17). For instance, for a PA of the maximum nonlinear order $M = 5$, an extra cancelling signal $C_5[k]$ for the fifth-order nonlinear SI is constructed in a similar way as $C_3[k]$ using (16). Subsequently, $C_5[k]$ is subtracted from the resulting signal of the third-order nonlinear cancellation in (17) to cancel the fifth-order nonlinear distortion.

B. COMPUTATION COMPLEXITY

It is worth noting that the complexity of the proposed blind cancellation approach is quite low due to the fact that it is not required to estimate the SI channel or the PA model coefficients. For the linear SI cancellation process, which is similar as the work in [36], the computation complexity is quite low, as analyzed in [36]. While for the nonlinear SI cancellation process, each nonlinear distortion of the PA is first transformed into a linear operation between the unknown nonlinear coefficients and the known transmitted signal in frequency domain as shown in (10). The associated computation complexity is also low and quite close to that of the linear SI cancellation process. Specifically, for the SI cancellation process in (14) and (17), only two multiplication and two addition processes are needed for the k-th symbol. For the recovery stage for the desired signal in (25) and (30), only four multiplication and four addition processes are needed for the k-th symbol. Also note that, as $X[k]/X[k-1]$, $X[k]/X[K]$, $A[k]/A[k-1]$, and $A[k]/A[K]$ in these processes are known to the local receiver, they can be pre-computed to reduce the calculation burden of the proposed approach. Thus, on average, only six multiplication and six addition processes are needed for each symbol.

V. VERIFICATIONS

A. SIMULATION CONDITION

For proof-of-concept evaluation, the effectiveness of the blind nonlinear SI cancellation is verified in terms of the computation complexity, the cancellation capability for the SI signal, and the BER of the desired signal. The cancellation capability is defined as

$$G = \frac{P_I + \sigma_N^2}{P_r + \sigma_N^2}, \tag{31}$$

where P_I, P_r and σ_N^2 are the powers of the received SI, the residual SI and the receiver noise, respectively. The simulation parameters are chosen from typical FD transceiver designs as shown in Table 1. At the transmitter side of the FD transceiver, the transmitted waveform is a 20-MHz OFDM signal composed of $N = 1200$ subcarriers with 16-QAM modulation. During the waveform generation, the N transmit symbols $\{X[k]\}_{k=0}^{N-1}$, are padded with a total number of 848 zeros to take advantage of the fast Fourier transform (FFT), as typically used in Long-Term Evolution (LTE) systems. Accordingly, the sampling rate of the transmitted waveform is $(1200 + 848) \times 15000 = 30.72$ Msps.

TABLE 1. System level parameters of a full-duplex transceiver.

Simulation Parameter	Value
Signal bandwidth	20 MHz
Modulation scheme	OFDM + 16QAM
Transmission power	10 dBm – 30 dBm
PA OIP3	40 dBm
Transmitter SNR	60 dB
Antenna isolation	30 dB
Analog cancellation	40 dB
ADC effective number of bits	11.5 bits
Desired signal power	−75 dBm
Receiver noise floor	−95 dBm

Subsequently, the generated waveform is first up-sampled by a factor of 8, with the sampling rate being increased to 245.76 Msps, to account for the seventh-order nonlinear distortion of the PA, which expands the bandwidth of the transmitted waveform to 140 MHz for a 20-MHz signal. The waveform is then sent to a PA model and amplified to power levels ranging from 10 dBm to 30 dBm to demonstrate different nonlinear distortions. The PA model used here is an MLM with a maximum nonlinear order of 7, whose nonlinear coefficients are extracted from a practical class-AB PA with a third-order intercept point (OIP3) of 40 dBm. Thus, ideally, the transmitter produces different nonlinear distortions ranging from −50 dBm to 10 dBm. The extracted MLM coefficients are listed as follows:

$$a_1 = 1.073 + 0.067j, \quad a_3 = 0.191 - 0.440j,$$
$$a_5 = -0.573 + 0.064j, \quad a_7 = 0.043 + 0.027j.$$

At the receiver side of the FD transceiver, the antenna isolation is configured to 30 dB due to the propagation attenuation between the local transmit and receive antennas, which is also a typical value considered in FD applications [5], [24], [32]. The SI channel and the channel between local transceiver and the remote transceiver are considered as single-path Rayleigh fading for simplicity. According to current FD transceiver designs [12]–[14], [33], the analog cancellation capability and the receiver noise floor used in the simulations are chosen to be 40 dB and −95 dBm, respectively. As analyzed in Section II, the analog cancellation process is simply modeled as an attenuation on the transmitted signal, which is a linear process on both the linear SI and nonlinear components as well as the transmitter noise. Thus, the linear SI, the nonlinear SI, and the transmitter noise are all attenuated by 40 dB. Accordingly, SI signal is within the dynamic range of ADC of the local receiver and can now be captured and processed in digital domain. However, even after the analog cancellation process, the nonlinear distortion would be still obvious as the transmission power increases. As shown in Fig. 3, when the transmission power increases to 30 dBm, the nonlinear distortion component of the residual SI will reach −60 dBm which is 35 dB above the receiver noise floor and 15 dB above the desired signal.

B. PROCEDURE

In the digital domain of the receiver, the received signal is first filtered by a low-pass filter whose bandwidth is chosen to be 30 MHz to mainly account for the in-band nonlinear distortions. The filtered signal is then down-sampled to 30.72 Msps before being aligned with the transmitted signal $x(n)$. FFT is then performed on the received sequence $\{r(n)\}_{n=0}^{N-1}$ to obtain the symbols in the frequency domain $\{R[k]\}_{k=0}^{N-1}$, which will be processed by the proposed blind cancellation approach to obtain the desired signal. To cancel the 7-order PA nonlinear distortions, a maximum order of 7 is considered during the proposed blind nonlinear SI cancellation, which performs four rounds of cancellation and recovery operations in total.

As comparisons, the conventional linear and nonlinear SI cancellations are also demonstrated, which are accomplished by three steps [12], [13]:

- S1 Estimating the linear SI channels and the nonlinear PA model coefficients in time domain;
- S2 Reconstructing the SI signal from the estimated SI channel and PA model;
- S3 Subtracting reconstructed SI from the digital received signal.

In the conventional nonlinear cancellation method, three groups of time-domain samples of different length L ($L = 10$, 100, and 1000, respectively) are used to estimate the SI channel and the PA coefficients with different estimation accuracies and complexities. During the training process the conventional nonlinear cancellation method, the SI channel and the PA nonlinearity are simply combined and modeled as an MLM, whose nonlinear order is also chosen to be 13 to

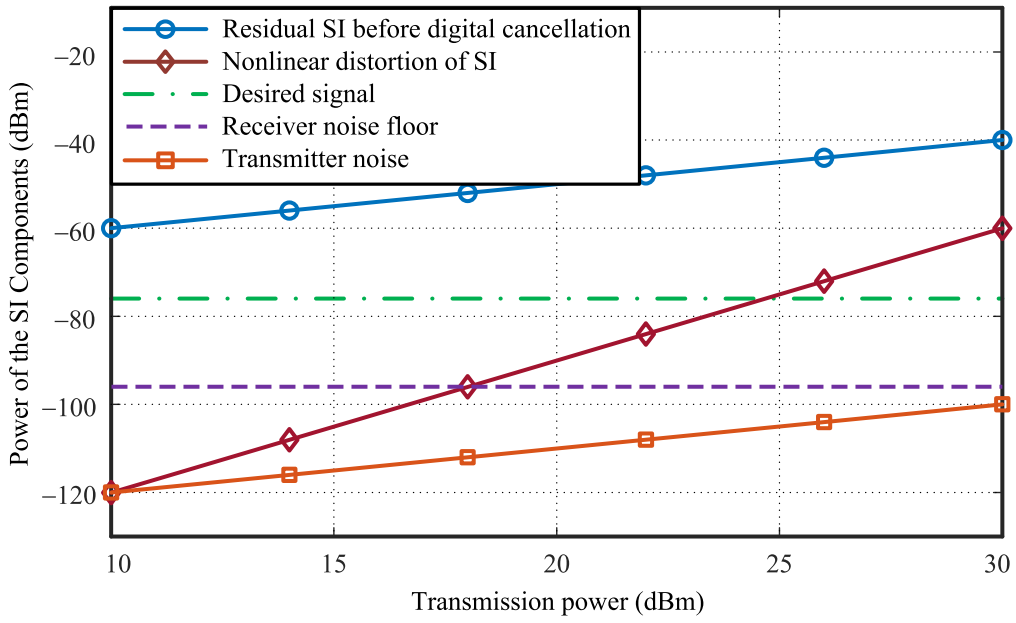

FIGURE 3. Power levels of different components of the received signal before digital nonlinear SI cancellation.

provide a fair comparison with our method as well as some redundancies for nonlinear model identification.

In our approach, the processing length K used in (14), (17), (25), and (30) is set to $K = N = 1200$. In the following, signal-to-noise ratio (SNR) is defined as the power ratio of the desired signal to the noise. As analyzed in Section II, both the SI signal $r_I(n)$ and the desired signal $r_U(n)$ are synchronized with the transmitted baseband signal $x(n)$, thus the CP insertion and removal processes are omitted for simplicity.

C. RESULTS FOR FREQUENCY FLAT CHANNEL

In this section, the performances of different SI cancellation methods are compared in terms of the computation complexity, the cancellation capability for the SI signal, residual SI power, and the BER of the desired signal.

1) COMPUTATION COMPLEXITY

In this simulation, the computation complexity is evaluated by the average time consumed to cancel the linear and nonlinear SI components within each symbol/sample of the received signal. For each SI cancellation method, the associated calculations are simulated to run over 10,000 symbols/samples to obtain the average time consume on each symbol/sample.

For the step S1 of the conventional method, the nonlinear model identification is implemented by using the LS algorithm. In this simulation, the LS algorithm involves some complicated calculations [18]. In the case of frequency flat SI channel model, matrix multiplication between a $4 \times L$ matrix and an $L \times 4$ matrix and matrix inversion of a 4×4 matrix are required.

As shown in Table 2, the computation complexity of the proposed blind nonlinear cancellation method is quite low and is even less than the step S2 and step S3 of the conventional nonlinear method. The computation complexity of the training process (model identification) of the conventional nonlinear SI cancellation method is extremely high and is at least 1,000 times over the proposed blind cancellation method. Thus, the computation complexity of the proposed blind nonlinear cancellation method is ignorable compared to the model identification process of the conventional nonlinear SI cancellation method, demonstrating stronger adaptation capability over the conventional method.

TABLE 2. Time consumptions of different SI cancelation methods under frequency flat channel.

Cancelation Method	Configuration	Time Consumed (μs)
Conv. nonlinear method	S1 with $L = 10$	21.569
	S1 with $L = 100$	26.359
	S1 with $L = 1000$	32.794
	S2 + S3	0.032
Prop. method	Cancelation & recovery	0.019

2) CANCELLATION CAPABILITY FOR THE SI

The cancellation capability comparisons between different cancellation methods are shown in Fig. 4. The cancellation capability of the linear method first raises linearly to 31 dB, then slightly raises to 34 dB, and eventually drops to 19 dB. When the transmission power ranges from 10 dBm to 15 dBm, the associated nonlinear SI is within the range from -120 dBm to -105 dBm at the receiver thus ignorable compared with the receiver noise floor of -95 dBm.

However, as the transmission power reaches 18 dBm, the nonlinear SI becomes −96 dBm and is comparable with the receiver noise floor, which shows some impacts on the linear cancellation capability. As the transmission power reaches 30 dBm, the nonlinear SI becomes −60 dBm, which is 35 dB above the receiver noise floor. As a consequence, the linear cancellation method fails to work properly and the cancellation capability dramatically drops to 19 dB.

The conventional nonlinear cancellation method [13] characterizes both the nonlinearity of the PA model and the SI channel response to mitigate the nonlinear SI, demonstrating good cancellation capability even when the transmission power reaches 30 dBm. During the nonlinear cancellation, a model identification process is required to extract both the SI channel response and the nonlinear coefficients, which requires L (processing length) samples to perform the LS algorithm. For the case with processing length $L = 10$, the processing length is too short to provide stable and effective estimation of the nonlinearity, resulting in poor cancellation of the SI signal. As the processing length increases to $L = 1000$, the cancellation capability significantly increases. However, more calculation complexity is introduced for implementing step S1 of the conventional nonlinear cancellation method, as listed in Table 2.

Alternatively, our blind nonlinear cancellation method, provides good cancellation performance for all the considered transmission power levels, which is even comparable to the conventional nonlinear cancellation method with high complexity (i.e., the case with $L = 1000$). Differently, the proposed method can be easily implemented with only a few multiplications and additions, as mentioned in Section III, given operations $X[k]/X[k-1]$, $X[k]/X[K]$, $A[k]/A[k-1]$, and $A[k]/A[K]$ in (14), (17), (25), and (30) of the proposed approach are known to the local receiver and can be pre-computed to further reduce the calculation burden.

3) BER OF THE DESIRED SIGNAL

Fig. 5 shows the BER comparisons between the three different SI cancellation methods, where the ideal BER of the case without SI is also shown for comparison. The BER of the conventional linear cancellation degrades fast with the increase of transmission power as expected, due to the presence of PA nonlinear distortion in the transmitter. The conventional nonlinear cancellation method with $L = 100$ and $L = 1000$ perform well with BER close to the ideal case without SI. For the particular configuration with $L = 10$, the processing length of the nonlinear model identification is too short to provide effective model identification results, thus fails to work properly.

For each power level, the BER of the proposed blind nonlinear cancellation is very close to that of the case without SI and keeps nearly unchanged with the transmission power. This trend indicates that the residual SI and the introduced interference by the proposed blind nonlinear SI cancellation method are small enough and thus would not degrade the decoding performance for the desired signal.

D. RESULTS FOR FREQUENCY SELECTIVE CHANNEL

In this section, the performances of different SI cancellation methods are compared under two frequency selective SI channels. The first SI channel (SI channel I) has 0.9 ns, 20 ns, 50 ns, 100 ns, and 200 ns delays with path loss being −30 dB, −75 dB, −85 dB, −95 dB, and −100 dB, respectively. While the second SI channel (SI channel II) has the same delays with path loss being −30 dB, −65 dB, −70 dB, −90 dB, and −100 dB, respectively. In these two SI channels, the path with 0.9 ns delay corresponds to the LOS SI path, while the others corresponds to the space multi-path reflections. These two power delay profiles are modified from the measurements in [6] and [37] to fit better the considered FD scenario with one strong LOS SI and few weak reflections.

TABLE 3. Time consumptions of different SI cancelation methods under frequency selective channels.

Cancelation Method	Configuration	Time Consumed
Conv. nonlinear method	S1 with $L = 10$	2.631 ms
	S1 with $L = 100$	3.789 ms
	S1 with $L = 1000$	6.782 ms
	S2 + S3	0.779 μs
Prop. method	Cancelation & recovery	0.019 μs

1) COMPUTATION COMPLEXITY

For conventional SI cancellation, more taps are used to model the frequency selective SI channel. In this simulation, the total number of the taps is chosen to be 50 to cover the maximum delay of the two SI channels. As a consequence, the total number of the nonlinear coefficients becomes $4 \times 50 = 200$. Accordingly, the LS algorithm needs to perform matrix multiplication between a $200 \times L$ matrix and an $L \times 200$ matrix and matrix inversion of a 200×200 matrix, which significantly increase the computation complexity. As shown in Table 3, the consumed time of the step S2 and S3 of the conventional nonlinear method is increased to be over 30 times than that of the proposed blind nonlinear cancellation method.

2) CANCELLATION CAPABILITY FOR THE SI

Fig. 6 shows the cancellation capability of the proposed blind nonlinear cancellation method under two frequency selective SI channels. The conventional linear method and the conventional nonlinear method with two different processing lengths (i.e., the cases with $L = 100$ and $L = 1000$) are also illustrated for comparisons. For different SI channels, the conventional linear and nonlinear methods demonstrate similar performances, thus, only the capabilities for SI channel I are illustrated for simplicity. By comparing Fig. 4 and Fig. 6, one can observe that the conventional nonlinear

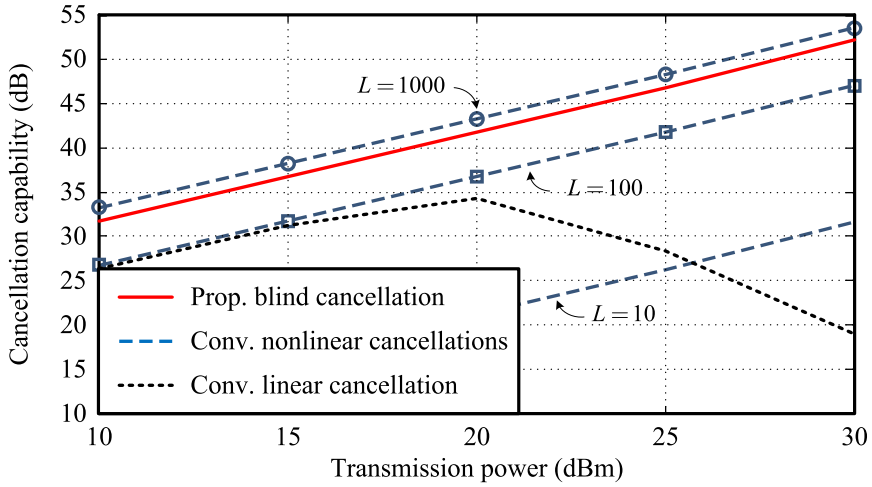

FIGURE 4. Cancellation capabilities of the SI signal for different SI cancellation methods.

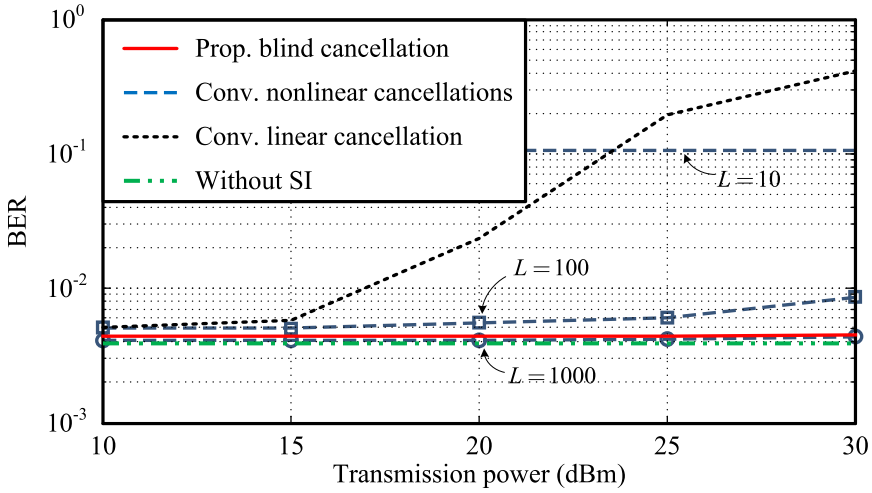

FIGURE 5. BERs of the desired signal from a remote user after different SI cancellation methods.

method demonstrates only a slight performance degradation of up to 2.4 dB in frequency selective channel.

While for the proposed blind nonlinear cancellation method, one can observe obvious performance drops of 5 dB and 10 dB for SI channel I and SI channel II, respectively. This is because when the SI channel becomes frequency selective, β in signal model (10) would become $\{\beta[k]\}_{k=0}^{N}$ denoting the joint frequency response of the SI channel and analog cancellation for the kth-subcarrier. Then simply using symbol on adjacent subcarrier $R[k-1]$ to cancel the SI within $R[k]$ would introduces an cancellation degradation due to the difference between $\beta[k-1]$ and $\beta[k]$. However, the proposed blind nonlinear cancellation method could still provide effective cancellation for both the linear SI and the nonlinear SI. Particularly, under SI channel I (frequency selective SI channel with one strong LOS component and weak space multi-path reflections), the proposed blind nonlinear method still outperforms the conventional nonlinear method of processing length $L = 100$, for all the considered power levels.

3) BER OF THE DESIRED SIGNAL

Fig. 7 shows the BER comparisons between the three different SI cancellation methods, where the ideal BER of the case without SI is also shown. For conventional nonlinear method, only the cases with processing lengths $L = 100$ and $L = 1000$ under SI channel I are illustrated for simplicity.

From Fig. 5 and Fig. 7, one can see that the proposed blind method suffers performance degradations as the frequency selectivity of the SI channel increases, which is consistent with the trend observed from Fig. 4 and Fig. 6. However, the proposed blind method can still provide good BERs under the two frequency selective SI channels. Particularly under SI channel I, the proposed blind method provides even better

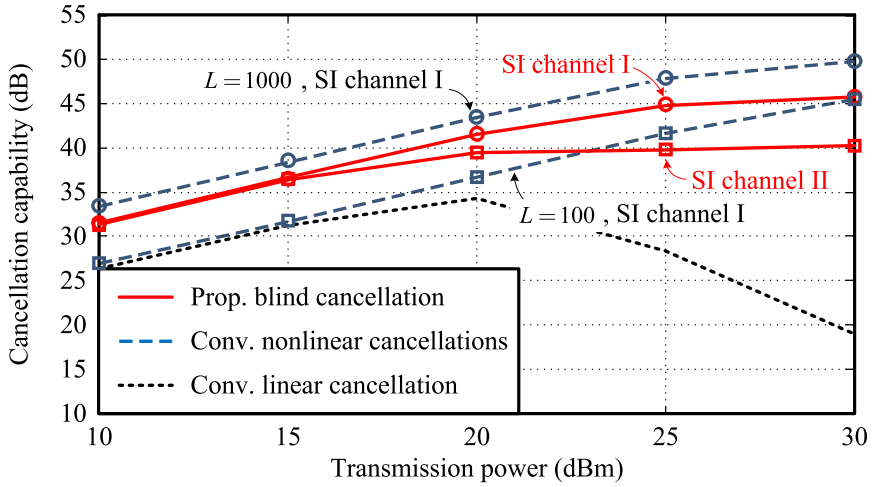

FIGURE 6. Cancellation capabilities of the SI signal for different SI cancellation methods under frequency selective SI channels.

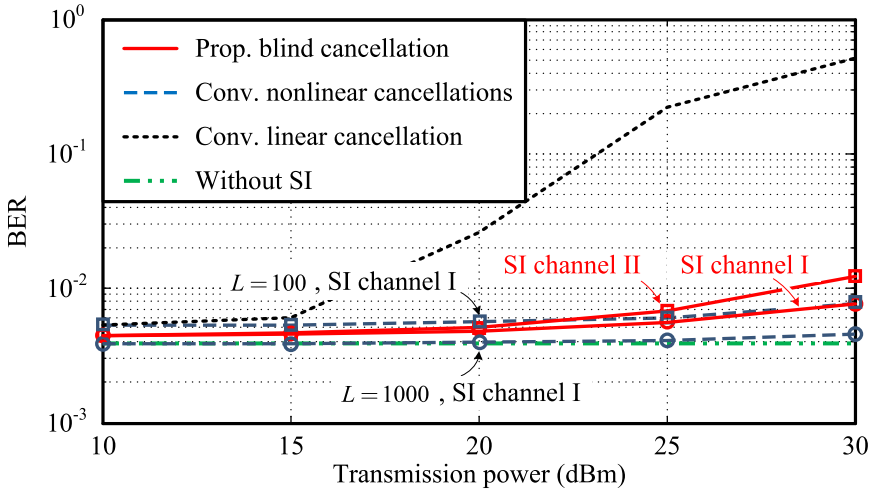

FIGURE 7. BERs of the desired signal from a remote user after different SI cancellation methods under frequency selective SI channels.

BERs compared with the conventional nonlinear method of processing length $L = 100$.

VI. CONCLUSION

In this work, a novel nonlinear SI cancellation method is proposed for high-power FD transceivers experiencing strong nonlinear distortions. This method consists of an SI cancellation process and a recovery process for the desired signal. The SI cancellation process uses the received symbols on two adjacent subcarriers in one OFDM symbol to cancel both the linear and nonlinear SI components without any estimation process. Subsequently, the recovery process is performed on the resulting signal to recover the desired signal and mitigate any impacts introduced by the nonlinear SI cancellation process. To the best of our knowledge, it is the first work to cancel the nonlinear SI signal without estimating the coefficients of the PA nonlinear model and the SI channel response. By employing this method, the SI is suppressed to near the receiver noise floor, and the BER of the signal-of-interest is close to that of the ideal case without SI, even under strong nonlinear distortions. Particularly, as no estimation process is required, this method demonstrates much lower computation complexity and simpler structure for implementation compared with conventional nonlinear SI cancellation method based on model estimation.

This proposed method provides a promising alternative solution for digital SI cancellation, particularly for high-power FD applications where the PA of the transmitter experiences strong nonlinear distortions. Future works will be performed to develop a more generalized algorithm to cover signals of wider bandwidth and PAs demonstrating strong memory effects, under frequency selective SI channels of strong space multi-path reflections. Testbed will be designed and experiments will be performed to verify its effectiveness.

REFERENCES

[1] J. Li, H. Zhang, and M. Fan, "Digital self-interference cancellation based on independent component analysis for co-time co-frequency full-duplex communication systems," *IEEE Access*, vol. 5, pp. 10222–10231, 2017.
[2] A. Sabharwal, P. Schniter, D. Guo, D. W. Bliss, S. Rangarajan, and R. Wichman, "In-band full-duplex wireless: Challenges and opportunities," *IEEE J. Sel. Areas Commun.*, vol. 32, no. 9, pp. 1637–1652, Sep. 2014.
[3] Y. Liu, X. Quan, W. Pan, and Y. Tang, "Digitally assisted analog interference cancellation for in-band full-duplex radios," *IEEE Commun. Lett.*, vol. 21, no. 5, pp. 1079–1082, May 2017.
[4] X. Quan, Y. Liu, S. Shao, C. Huang, and Y. Tang, "Impacts of phase noise on digital self-interference cancellation in full-duplex communications," *IEEE Trans. Signal Process.*, vol. 65, no. 7, pp. 1881–1893, Apr. 2017.
[5] M. S. Sim, M. Chung, D. Kim, J. Chung, D. K. Kim, and C.-B. Chae, "Nonlinear self-interference cancellation for full-duplex radios: From link-level and system-level performance perspectives," *IEEE Commun. Mag.*, vol. 55, no. 9, pp. 158–167, Jun. 2017.
[6] Y. Liu, P. Roblin, X. Quan, W. Pan, S. Shao, and Y. Tang, "A full-duplex transceiver with two-stage analog cancellations for multipath self-interference," *IEEE Trans. Microw. Theory Techn.*, vol. 65, no. 12, pp. 5263–5273, Dec. 2017.
[7] J. Tamminen *et al.*, "Digitally-controlled RF self-interference canceller for full-duplex radios," in *Proc. Eur. Signal Process. Conf.*, Aug. 2016, pp. 783–787.
[8] A. Sahai, G. Patel, and A. Sabharwal, "Pushing the limits of full-duplex: Design and real-time implementation," Rice Univ., Houston, TX, USA, Tech. Rep. TREE1104, 2011.
[9] D. Korpi *et al.*, "Full-duplex mobile device: Pushing the limits," *IEEE Commun. Mag.*, vol. 54, no. 9, pp. 80–87, Sep. 2016.
[10] M. Heino *et al.*, "Recent advances in antenna design and interference cancellation algorithms for in-band full duplex relays," *IEEE Commun. Mag.*, vol. 53, no. 5, pp. 91–101, May 2015.
[11] M. Chung, M. S. Sim, J. Kim, D. K. Kim, and C.-B. Chae, "Prototyping real-time full duplex radios," *IEEE Commun. Mag.*, vol. 53, no. 9, pp. 56–63, Sep. 2015.
[12] M. Jain *et al.*, "Practical, real-time, full duplex wireless," in *Proc. Annu. Int. Conf. Mobile Comput. Netw. (ACM Mobicom)*, Las Vegas, NV, USA, Sep. 2011, pp. 301–312.
[13] D. Bharadia, E. McMilin, and S. Katti, "Full duplex radios," in *Proc. ACM SIGCOMM*, Hong Kong, 2013, pp. 375–386.
[14] D. Korpi, L. Anttila, and V. Syrjälä, and M. Valkama, "Widely linear digital self-interference cancellation in direct-conversion full-duplex transceiver," *IEEE J. Sel. Areas Commun.*, vol. 32, no. 9, pp. 1674–1687, Sep. 2014.
[15] L. Anttila, D. Korpi, E. Antonio-Rodríguez, R. Wichman, and M. Valkama, "Modeling and efficient cancellation of nonlinear self-interference in MIMO full-duplex transceivers," in *Proc. IEEE Globecom Workshops (GC Wkshps)*, Austin, TX, USA, Dec. 2014, pp. 777–783.
[16] E. Ahmed, A. Eltawil, and A. Sabharwal, "Self-interference cancellation with nonlinear distortion suppression for full-duplex systems," in *Proc. Asilomar Conf. Signals, Syst. Comput.*, Pacific Grove, CA, USA, Nov. 2013, pp. 1199–1203.
[17] L. Anttila, D. Korpi, V. Syrjälä, and M. Valkama, "Cancellation of power amplifier induced nonlinear self-interference in full-duplex transceivers," in *Proc. Asilomar Conf. Signals, Syst. Comput.*, Pacific Grove, CA, USA, Nov. 2013, pp. 1193–1198.
[18] M. Chung, M. S. Sim, D. K. Kim, and C.-B. Chae, "Compact full duplex MIMO radios in D2D underlaid cellular networks: From system design to prototype results," *IEEE Access*, vol. 5, pp. 16601–16617, 2017.
[19] Y. Liu, X. Quan, W. Pan, S. Shao, and Y. Tang, "Performance analysis of direct-learning digital predistortion with loop delay mismatch in wideband transmitters," *IEEE Trans. Veh. Technol.*, vol. 65, no. 9, pp. 7078–7089, Sep. 2016.
[20] L. Ding *et al.*, "A robust digital baseband predistorter constructed using memory polynomials," *IEEE Trans. Commun.*, vol. 52, no. 1, pp. 159–165, Jan. 2004.
[21] F. Jiang and A. L. Swindlehurst, "Optimization of UAV heading for the ground-to-air uplink," *IEEE J. Sel. Areas Commun.*, vol. 30, no. 5, pp. 993–1005, Jun. 2012.
[22] M. Mozaffari, W. Saad, M. Bennis, and M. Debbah, "Unmanned aerial vehicle with underlaid device-to-device communications: Performance and tradeoffs," *IEEE Trans. Wireless Commun.*, vol. 15, no. 6, pp. 3949–3963, Jun. 2016.
[23] H. Rahul, H. Hassanieh, and D. Katabi, "SourceSync: A distributed wireless architecture for exploiting sender diversity," in *Proc. ACM SIGCOMM*, New Delhi, India, Aug. 2010, pp. 171–182.
[24] E. Ahmed and A. M. Eltawil, "All-digital self-interference cancellation technique for full-duplex systems," *IEEE Trans. Wireless Commun.*, vol. 14, no. 7, pp. 3519–3532, Jul. 2015.
[25] S. Zhang, S. C. Liew, and H. Wang, "Blind known interference cancellation," *IEEE J. Sel. Areas Commun.*, vol. 31, no. 8, pp. 1572–1582, Aug. 2013.
[26] E. Ahmed and A. M. Eltawil, "On phase noise suppression in full-duplex systems," *IEEE Trans. Wireless Commun.*, vol. 14, no. 3, pp. 1237–1251, Mar. 2015.
[27] V. Syrjala, M. Valkama, L. Anttila, T. Riihonen, and D. Korpi, "Analysis of oscillator phase-noise effects on self-interference cancellation in full-duplex OFDM radio transceivers," *IEEE Trans. Wireless Commun.*, vol. 13, no. 6, pp. 2977–2990, Jun. 2014.
[28] Q. Huang, M. Ghogho, J. Wei, and P. Ciblat, "Practical timing and frequency synchronization for OFDM-based cooperative systems," *IEEE Trans. Signal Process.*, vol. 58, no. 7, pp. 3706–3716, Jul. 2010.
[29] M. Morelli, "Timing and frequency synchronization for the uplink of an OFDMA system," *IEEE Trans. Commun.*, vol. 52, no. 2, pp. 296–306, Feb. 2004.
[30] L. Sanguinetti and M. Morelli, "An initial ranging scheme for the IEEE 802.16 OFDMA uplink," *IEEE Trans. Wireless Commun.*, vol. 11, no. 9, pp. 3204–3215, Sep. 2012.
[31] Q. Sun, D. C. Cox, H. C. Huang, and A. Lozano, "Estimation of continuous flat fading MIMO channels," *IEEE Trans. Wireless Commun.*, vol. 1, no. 4, pp. 549–553, Oct. 2002.
[32] D. Korpi, T. Huusari, Y.-S. Choi, L. Anttila, S. Talwar, and M. Valkama, "Digital self-interference cancellation under nonideal RF components: Advanced algorithms and measured performance," in *Proc. IEEE 16th Int. Workshop Signal Process. Adv. Wireless Commun. (SPAWC)*, Stockholm, Sweden, Jun./Jul. 2015, pp. 286–290.
[33] K. E. Kolodziej, B. T. Perry, and J. G. McMichael, "Multitap RF canceller for in-band full-duplex wireless communications," *IEEE Trans. Wireless Commun.*, vol. 15, no. 6, pp. 4321–4334, Jun. 2016.
[34] Y. Liu, W. Ma, X. Quan, W. Pan, K. Kang, and Y. Tang, "An architecture for capturing the nonlinear distortion of analog self-interference cancellers in full-duplex radios," *IEEE Microw. Wireless Compon. Lett.*, vol. 27, no. 9, pp. 845–847, Aug. 2017.
[35] Y. Liu, W. Pan, S. Shao, and Y. Tang, "A general digital predistortion architecture using constrained feedback bandwidth for wideband power amplifiers," *IEEE Trans. Microw. Theory Techn.*, vol. 63, no. 5, pp. 1544–1555, May 2015.
[36] D. Liu, B. Zhao, F. Wu, S. Shao, X. Pu, and Y. Tang, "Semi-blind SI cancellation for in-band full-duplex wireless communications," *IEEE Commun. Lett.*, vol. 22, no. 5, pp. 1078–1081, May 2018.
[37] X. Wu, Y. Shen, and Y. Tang, "The power delay profile of the single-antenna full-duplex self-interference channel in indoor environments at 2.6 GHz," *IEEE Antennas Wireless Propag. Lett.*, vol. 13, pp. 1561–1564, 2014.

XIN QUAN (S'13) was born in Shijiazhuang, Hebei, China, in 1988. She received the B.E. degree in communication engineering from Yanshan University, Qinhuangdao, China, in 2010, and the M.S. degree in communication and information system from University of Science and Technology of China, Chengdu, China, in 2013, where she is currently pursuing the Ph.D. degree.

From 2014 to 2015, she was a Visiting Scholar with the Department of Electrical and Computer Engineering, The Ohio State University, Columbus, USA. Her research interests include channel estimation, interference suppression, full-duplex wireless communication, nonlinear distortion mitigation, and signal processing in wireless communications.

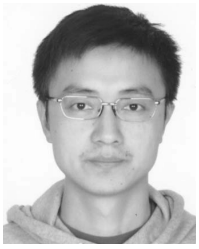

YING LIU (S'13–M'16) received the B.E. and the M.S. degrees in communication engineering and the Ph.D. degree in communication and information system from the University of Electronic Science and Technology of China (UESTC) in 2008, 2011, and 2016, respectively. He is currently an Assistant Professor with the National Key Laboratory of Science and Technology on Communications, UESTC, where he is also a Post-Doctoral Researcher with the School of Electronic Engineering.

From 2014 to 2015, he was a Visiting Scholar with the Department of Electrical and Computer Engineering, The Ohio State University, Columbus, USA. His research interests include nonlinear modeling, digital predistortion, full-duplex wireless communications, and signal processing in wireless communications.

DONG CHEN received the B.S. degree in communication engineering from the University of Electronic Science and Technology of China, Chengdu, China, in 2013, where he is currently pursuing the Ph.D. degree. His research interests include modeling of on-chip devices, CMOS RF and mm-wave integrated circuits, and power amplifier design.

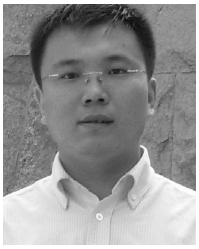

SHIHAI SHAO (GS'05–M'10) was born in Fushun, Liaoning, China, in 1980. He received the B.E. and Ph.D. degrees in communication and information system from the University of Electronic Science and Technology of China, Chengdu, China, in 2003 and 2008, respectively.

Since 2008, he has been a Professor with the National Key Laboratory of Science and Technology on Communications, University of Electronic Science and Technology of China. His research interests include full-duplex communications, signal processing in wireless communications, spread spectrum, and MIMO detection.

YOUXI TANG was born in Xinyang, Henan, China, in 1964. He received the B.E. degree in radar engineering from the College of PLA Ordnance, Shijiazhuang, China, in 1985, and the M.S. and Ph.D. degrees in communications and information systems from the University of Electronic Science and Technology of China, Chengdu, China, in1993 and 1997, respectively.

From 1998 to 2000, he was a Program Manager with Huawei Technologies Company Ltd., Shanghai, China, where he was involved in the area of IS-95 mobile communications and third-generation mobile communications. Since 2000, he has been a Professor with the National Key Laboratory of Science and Technology on Communications, University of Electronic Science and Technology of China. His general research interests include spread spectrum systems and wireless mobile systems with emphasis on signal processing in communications.

KAI KANG (M'08) received the B.Eng. degree in electrical engineering from Northwestern Polytechnical University, China, in 2002, and the joint Ph.D. degree from the National University of Singapore, Singapore, and École supérieure d'électricité, France, in 2008.

From 2006 to 2010, he was a Senior Research Engineer with the Institute of microelectronics, A*STAR, Singapore. Since 2011, he has been with the University of Electronic Science and Technology of China, where he is currently a Professor and an Associate Dean with the School of Electronic Engineering. His research interests are RF and mm-Wave integrated circuits design and modeling of on-chip devices.